

Comparative theoretical study of single-wall carbon and boron-nitride nanotubes

Brahim Akdim and Ruth Pachter

Air Force Research Laboratory, Materials and Manufacturing Directorate, AFRL/MLPJ, WPAFB, Ohio 45433

Xiaofeng Duan

Major Shared Resource Center for High Performance Computing, ASC/HP, WPAFB, Ohio 45433

W. Wade Adams

Rice University, Center for Nanoscale Science and Technology, Houston, Texas 77005

(Received 13 January 2003; published 6 June 2003)

We present a comprehensive comparative study of properties of BN and C nanotubes using a full potential linear combination of atomic orbitals approach, as well as a planewave pseudopotential method. This paper covers our results on the structural, mechanical, vibrational, and electronic properties, examining in detail the effects of intertube coupling. Structural aspects and mechanical properties are discussed and compared in BN and C nanotubes, and to experiment. Upshifts in the values of the radial breathing modes, due to intertube coupling, are found to be small and systematic, about 2% in zigzag nanotubes, and varying from 2 to 7% in armchair tubes, for both materials. Finally, the effects of intertube interactions on the van Hove singularities are discussed.

DOI: 10.1103/PhysRevB.67.245404

PACS number(s): 61.46.+w, 62.25.+g, 73.22.Gk, 78.30.Na

I. INTRODUCTION

From the time of their discovery, carbon (C)¹ and boron-nitride (BN)² nanotubes (BN-NT's and CNT's) have been receiving ever-increasing interest due to their novel properties and potential application in nanodevices. It is well established that CNT's can be either metallic or semiconducting, depending on the tube chirality and diameter, suggesting a variety of nanoelectronics applications.³⁻⁶ Furthermore, the high stiffness demonstrated experimentally by Young's moduli and tensile strength^{7,8} measurements, and by theoretical predictions⁹⁻¹¹ are notable, extending their potential applications, for example, to composite reinforced materials;¹² other application areas are being explored as well, such as hydrogen storage,¹³ or field emission;¹⁴⁻¹⁶ all of which have been recently summarized.¹⁷ BN-NT's are also interesting materials, due to their constant wide band gap (5.5 eV),¹⁸ independent of chirality and diameter, and in their ability to sustain heat. It has been shown recently that BN-coated CNT's demonstrate better field emission¹⁹ than as-produced CNT's.

Resonant Raman spectroscopy has become a promising technique in probing and characterizing the structure of nanotubes,^{20,21} which can be explained in terms of models that take into account the valence π and conduction π^* energy bands. The strong resonance Raman effect in nanotubes permits the study of their optical and electronic properties, which occurs between the singularities of the conduction and valence bands, and previous studies established a relationship with tube diameter.²¹⁻²⁴ However, relatively simplistic models may not be appropriate to predict RBM's, especially for small diameter tubes, and to provide insight into the effects of intertube interactions. Indeed, recently a study of single-wall carbon nanotube properties [C(n,n) and C($n,0$), $n=(4,6,8,10)$], was carried out,²⁵ where CNT's were modeled as isolated tubes or crystalline ropes, using a full-

potential linear combination of atomic orbitals (FP-LCAO) density functional theory approach. Although the full potential all-electron scheme is computationally intensive, the accuracy in modeling single-wall CNT's was evident in comparison to other theoretical work and experiment. Moreover, previous high-level theoretical calculations^{10,11} have been rather limited, and a comprehensive study using highly accurate methods, to validate an approach for a reliable prediction of RBM's in CNT's and BN-NT's, has not been carried out thus far. In this paper, we report an extensive and rigorous investigation using the all-electron LCAO and plane-wave pseudopotential methods (PW-PP). Calculated Young's moduli of CNT's are found to be in excellent agreement with recent experimental measurements⁷ and in light of these newly reported results, it is suggested that our calculated values for BN-NT's are also appropriately estimated. For the RBM's of CNT's, we validated our fitting constants by calculating the value of the RBM of an isolated large diameter C(20,20) nanotube, and compared it with the extrapolated value; we also fitted our RBM results to the suggested model by Bachilo *et al.*²⁴ Although we obtained excellent agreement with the fitted constant,²⁴ the proposed model does not hold for a large radius tube. Finally, we studied the effects of intertube interactions on the van Hove singularities (vHS) of CNT's, and calculated the ratio (E_{22}/E_{11}) to be in good agreement with recent experimental data.²⁶

II. COMPUTATIONAL DETAILS

FP-LCAO and PW-PP schemes, using DMOL3 and CASTEP,²⁷ were applied, adopting the generalized gradient approximation (GGA), with the Perdew and Wang²⁸ exchange-correlation functional and a double-numeric basis set. A hexagonal symmetry of order 8 with inversion was

TABLE I. Structural parameters of CNT's in crystalline-rope (rope) form and as isolated (isol.) tubes. Units are in Å.

	C(4,0)		C(6,0)		C(4,4)		C(8,0)		C(10,0)		C(6,6)		C(8,8)		C(10,10)	
	Rope	Isol.	Rope	Isol.	Rope	Isol.	Rope	Isol.	Rope	Isol.	Rope	Isol.	Rope	Isol.	Rope	Isol.
Horizontal bonds	1.460	1.463	1.435	1.435	1.421	1.421	1.422	1.425	1.421	1.420	1.415	1.415	1.413	1.413	1.412	1.412
Vertical bonds	1.400	1.398	1.405	1.404	1.418	1.417	1.411	1.409	1.411	1.411	1.417	1.417	1.416	1.416	1.414	1.414
R_{average}	1.660	1.665	2.402	2.399	2.746 ^a	2.746	3.158	3.160	3.933 ^c	3.929	4.070 ^e	4.077	5.420 ^g	5.416	6.760 ⁱ	6.761
Intertube distance	6.030		7.980		8.600		9.490		11.040		11.200		13.900		16.600	
$2R_{\text{average}} + 3.4$	6.720		8.200		8.900 ^b		9.720		11.270 ^d		11.540 ^f		14.240 ^h		16.920 ^j	

^a[2.794 (Ref. 11)].^b[8.990 (Ref. 11)].^c[3.979 (Ref. 11), 3.955 (Ref. 10)].^d[11.360 (Ref. 11), 11.310 (Ref. 10)].^e[4.140 (Ref. 11), 4.100 (Ref. 10)].^f[11.680 (Ref. 11), 11.600 (Ref. 10)].^g[5.498 (Ref. 11)].^h[14.400 (Ref. 11)].ⁱ[6.864 (Ref. 11), 6.800 (Ref. 10)].^j[17.130 (Ref. 11), 17.000 (Ref. 10)].

used to reduce computational time. Structural, mechanical, and vibrational properties were calculated using the FP-LCAO scheme, setting the atomic cutoff radius to 10.4 (a.u.). The k points sampling in the Brillouin zone were generated by the Monkhorst-Pack scheme, employing 15 k points for the crystalline rope (bundle) and 5 k points for an isolated tubule. In the case of electronic properties, we employed the PW-PP approach, with a planewave kinetic energy cutoff of 280 (eV), using 32 k points along the tube axis. Note that the geometry and cell parameters were optimized in all calculations (details are given elsewhere²⁵). In this work, the use of PW-PP, for the electronic structure calculations, is due to the flexibility available in the PW-PP codes in selecting the k points along the desired symmetry lines of the irreducible Brillouin zone. It should be noted that our GGA calculations, performed using a PW exchange-correlation functional, do not fully account for dispersion forces.^{29–31} Further evaluation of intertube interactions, possibly using asymptotically corrected functionals, would be advantageous.

III. RESULTS AND DISCUSSION

A. Structural parameters

The structural parameters of CNT's and BN-NT's are listed in Tables I and II, respectively, showing a small effect of intertube interactions. The intertube interaction

energies of CNT's were also calculated and found to be, on average, 0.2 and 0.17 eV/Å, for the zigzag and armchair tubes, respectively, in good agreement with previous theoretical work.³² As expected, the buckling in BN-NT's, evaluated by structure relaxation, leads to an outer and inner radius formed by nitrogen and boron atoms, respectively.¹⁰ This buckling is shown to be inversely proportional to the tube radius (Fig. 1), but does not depend on tube chirality. For the tubes considered in this work, we observed a 66% reduction in the buckling from BN(4,0) to BN(10,10) tubes. Figures 2 and 3 list bondlength changes of CNT's and BN-NT's, respectively, as a function of tube radius, for both horizontal (h) and vertical (v) bonds; h is in the direction of the circumference of the tube and v is parallel to the tube axis. The accuracy of bondlengths (Tables I and II) is important, as it is known that such small variations may affect properties, such as the vibrational frequencies.³³ Although the bondlengths in BN-NT's appear to have the same behavior as in covalently bonded CNT's, their variations with tube radius is small, compared to the bonding in CNT's, which may be due to the buckling. The horizontal and vertical bonds are found to be comparable in armchair tubes, with average values of 1.415 and 1.438 Å, for CNT's and BN-NT's, respectively, whereas in zigzag tubes, these bonds have an opposite behavior with respect to the tube radius, namely, an increase of the h bond while the v bond decreases for small radii

TABLE II. Structural parameters of BN-NT's in crystalline-rope (rope) form and as isolated (isol.) tubes. Units are in Å.

	BN(6,0)		BN(8,0)		BNC(9,0)		BN(6,6)		BNC(8,8)		BN(9,9)		BN(10,10)	
	Rope	Isol.	Rope	Isol.	Rope	Isol.	Rope	Isol.	Rope	Isol.	Rope	Isol.	Rope	Isol.
Horizontal bonds	1.454	1.454	1.449	1.447	1.448	1.446	1.442	1.441	1.440	1.441	1.441	1.439	1.437	1.437
Vertical bonds	1.437	1.437	1.438	1.438	1.439	1.438	1.454	1.440	1.442	1.442	1.442	1.441	1.438	1.438
R_N	2.487	2.485	3.186	3.185	3.649	3.642	4.180	4.177	5.537	5.546	6.216	6.222	6.887	6.888
R_B	2.393	2.393	3.253	3.254	3.593	3.582	4.125	4.125	5.499	5.507	6.185	6.188	6.858	6.858
Intertube distance	8.300		9.500		10.100		11.200		14.000		15.200		16.700	
$2R_N + 3.4$	8.370		9.770		10.700		11.760		14.470		15.830		17.170	

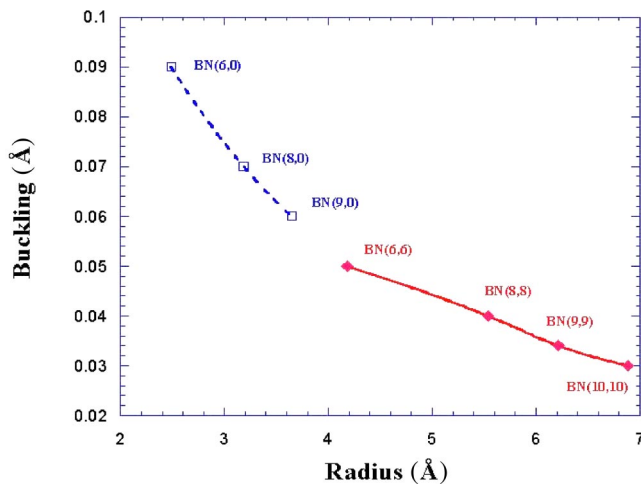


FIG. 1. Buckling of BN-NT's as a function of tube radius. The solid and dashed lines connecting the square symbols are for the purpose of visualization.

tubes. The small changes in bond lengths in armchair tubes may indicate a small hybridization of the π bond,¹¹ while in the zigzag tubes a strong rehybridization is evident, particularly for small radii tubes. This argument is further supported by our Young's moduli results. The converged bondlengths in CNT's and BN-NT's, agree well with the experimental data for a carbon sheet (1.419 Å)³⁴ and hexagonal BN (1.446 Å),³⁵ respectively.

B. Mechanical properties

The first measurement of Young's modulus for CNT's was performed by Treacy *et al.*³⁶ by applying the thermal vibrational amplitude technique, obtaining a value of (1.8 ± 1.4) TPa for multiwall CNT's; Krishnan *et al.*³⁷ measured a value in the range of (1.3–0.4, 1.3+0.6) TPa using the same technique; while Salvétat and co-workers³⁸ reported a value of (1.28 ± 0.58) TPa for single-wall bundles using an AFM with a special substrate to allow for a direct measurement. The most recent experiment⁷ reported a tensile strength and a

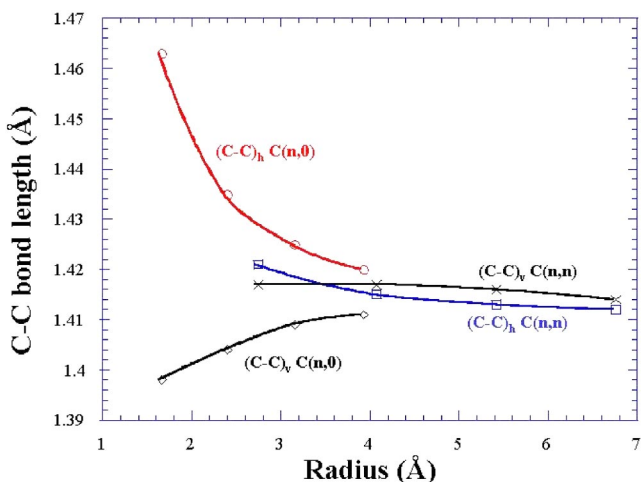


FIG. 2. Bondlengths of CNT's as a function of tube radius.

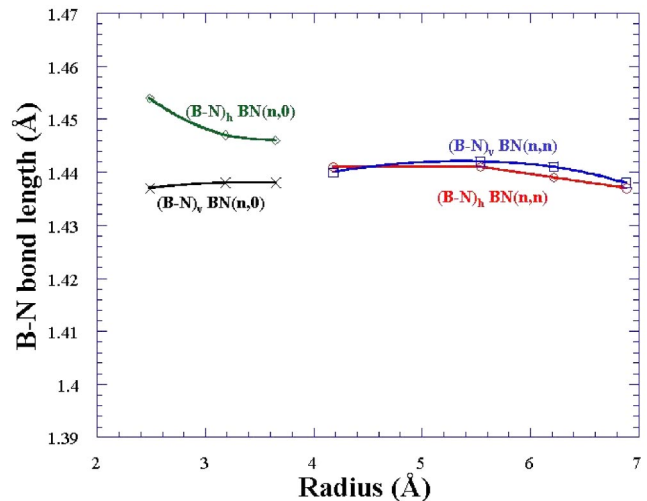


FIG. 3. Bondlengths of BN-NT's as a function of tube radius.

Young's modulus for CNT's to be 0.15 and 0.9 TPa, respectively. For BN-NT's, Young's modulus was measured³⁹ with the thermal vibrational amplitude technique, reporting a value of (1.20 ± 0.24) TPa.

According to elastic theory, Young's modulus (YM) involves a wall thickness definition, which has been controversial for single wall carbon nanotubes. Yakobson *et al.*⁸ used a value of 0.6 Å, leading to an unrealistic YM value (~5 TPa), as compared to experiment. Others^{9–11} have adopted the graphite interlayer value (3.4 Å) as the wall thickness, providing more realistic results. Using average optimized intertube distances of CNT's (3.07 Å) and BN-NT's (2.95 Å), in the calculation of YM's, will result in 15 and 20% upshifts, respectively, compared to those calculated using the 3.4 Å graphite interlayer value (which we used for comparison with other studies). However, the YM values of CNT's will still remain higher than those of BN-NT's, preserving the relative strength between these materials, as expected. Figure 4 illustrates the trend

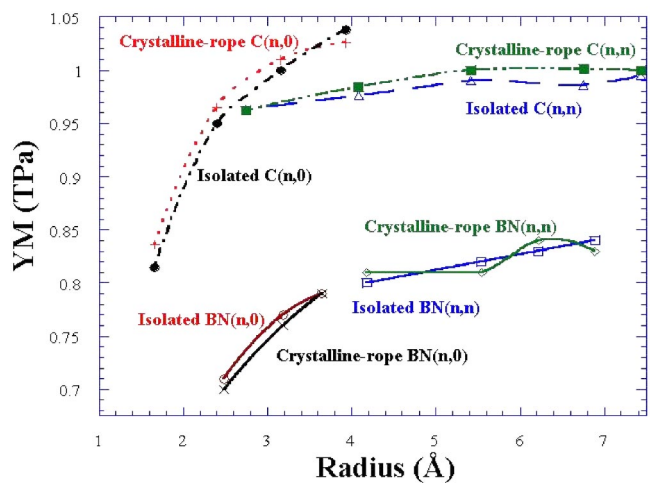


FIG. 4. CNT's and BN-NT's Young's moduli of isolated tubes and crystalline ropes as a function of tube radius.

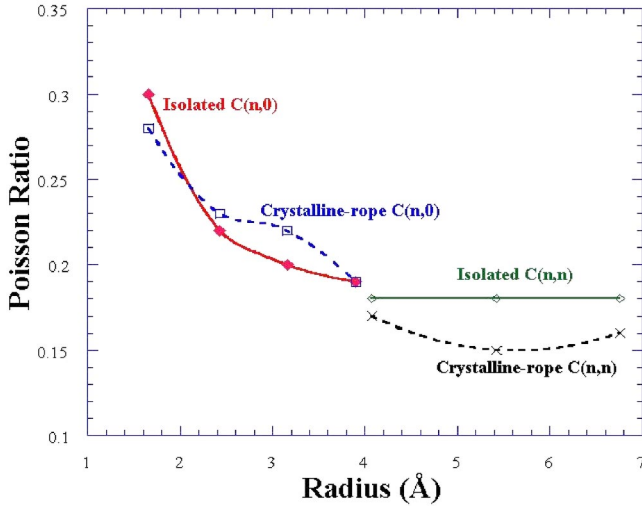


FIG. 5. CNT's Poisson ratio of isolated (solid line) tubes and crystalline ropes (dashed lines) as a function of tube radius.

in our calculated Young's moduli, as a function of tube radius. In general, intertube interactions do not alter Young's moduli results for C and BN nanotubes. For CNT's, we show a good agreement (see Table III) with a recent experimental value of 0.9 TPa,⁷ where our largest value is within 25% of experiment. Lu,⁹ using the force-constant model, obtained a closer value to experiment of 0.97 TPa;⁷ however, his predicted Young's moduli are independent of tube radius and chirality. Hernandez *et al.*¹⁰ reported results from a tight-binding study, which are higher by 35% than the recent reported data.⁷ We also find that Young's moduli depend on chirality in CNT's. In BN-NT's, our results are within the lower error bracket of the available data.³⁹ However, since BN-NT's are softer than CNT's, and in light of the

TABLE III. Young's moduli (YM, TPa) ($YM=(1/V_0) \times (\partial^2 E / \partial \epsilon^2)$, where, $V_0=2\pi L \delta R$; δR is the edge to edge intertube separation; L unit cell length, and R radius of the tube; $\delta R=3.4 \text{ \AA}$ for C and BN) for C and BN nanotubes.

Chirality	C		BN	
	Rope	Isol.	Rope	Isol.
(4,0)	0.82	0.84		
(6,0)	0.95	0.97	0.70	0.71
(4,4)	0.96	0.96		
(8,0)	1.01	1.01	0.77	0.77
(9,0)			0.79	0.79
(10,0)	1.04	1.03		
		[0.97 (Ref. 10), 1.22 (Ref. 11)]		
(6,6)	0.98	0.98	0.80	0.81
		[1.22 (Ref. 11)]	[0.87 (Ref. 11)]	
(8,8)	1.00	0.99	0.82	0.80
(9,9)			0.83	0.84
(10,10)	1.00	0.99	0.84	0.83
		[0.97 (Ref. 10), 1.24 (Ref. 11)]		

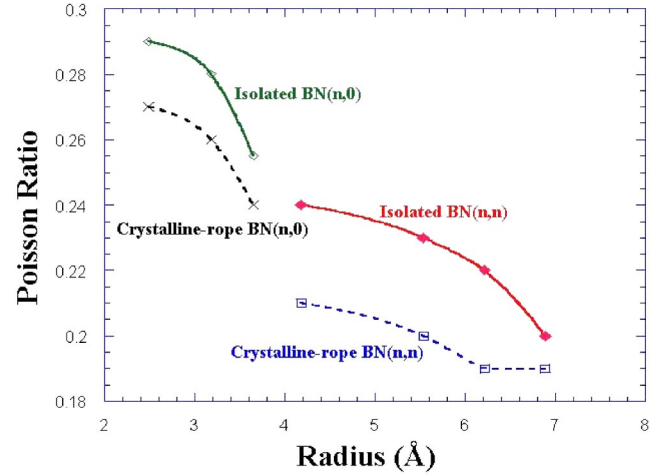


FIG. 6. BN-NT's Poisson ratio of isolated (solid line) tubes and crystalline ropes (dashed lines) as a function of tube radius.

new results for CNT's,⁷ our values can be considered to be in the right range. Our calculated results also show the curvature effect, that is, a decrease in strength for small radii tubes, in agreement with a previous theoretical study.¹⁰ The effect of the curvature is rather pronounced in zigzag nanotubes, suggesting a strong rehybridization of the π bond. These results are consistent with previous theoretical work on curvature effects.^{40,41}

Poisson ratio results provide insight on the tubes response to an external force, plotted in Figs. 5 and 6, for CNT's and BN-NT's, respectively. The results are found to depend on the tube radius, where small radii tubes have a higher response to axial strain. Furthermore, our findings indicate that in general BN-NT's are more sensitive to an external force than CNT's. With the exception of zigzag-CNT's, we note that the intertube interactions slightly decrease the sensitivity of tubes subject to axial strain.

C. Radial breathing modes and electronic density of states

Theoretical⁴² and experimental^{5,43,44} studies of RBM's for CNT's are well known and shown to be proportional to A/d , where d (nm) is the diameter and $A(\text{cm}^{-1} \text{ nm})$ a fitting constant. Dresselhaus *et al.*²¹ estimated an experimental value for A of $248 (\text{cm}^{-1} \text{ nm})$ for isolated tubes. Alvarez *et al.*⁴⁵ calculated $(232/d + 6.5)(\text{cm}^{-1})$ for bundled tubes, obtained by a tight-binding approach that includes the Lennard-Jones potential. Bandow *et al.*,⁴⁶ using a force constant model, have obtained $(223.75/d)(\text{cm}^{-1})$ for tube bundles of various chiralities. Sauvajol and co-workers, through generalized tight-binding molecular dynamics calculations, including also a Lennard-Jones potential to account for van der Waals (vdW) interactions, obtained a slightly different model for bundled tubes, namely, (A/d^α) , where α was found to be 0.93. Recently, Bachilo *et al.*²⁴ have fitted their results for isolated semiconducting tubes to $(223.5/d + 12.5)(\text{cm}^{-1})$, where $12.5 (\text{cm}^{-1})$ is a constant that gives the best r.m.s. error to the experimental data. These

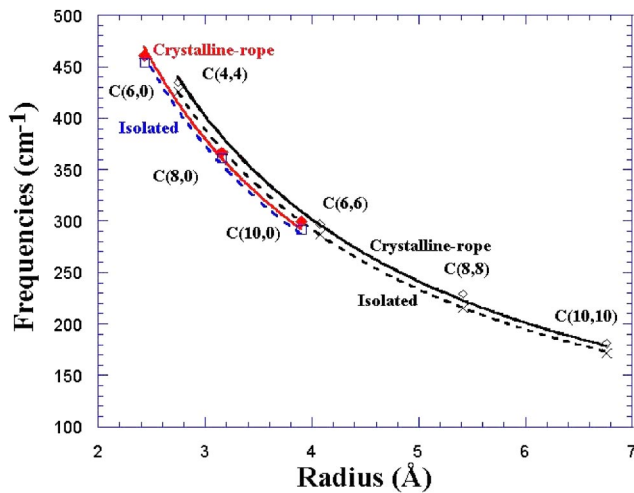


FIG. 7. FP-LCAO CNT's RBM's of isolated (dashed lines) tubes and crystalline ropes (solid lines) as a function of tube radius.

models assume the universal trend of (A/d) , independent of the chiral angle. A more complicated expression of the RBM was adopted by Kuzmany *et al.*⁴⁷ to predict the up shift for tube bundles $[234/d + C(N,d)](\text{cm}^{-1})$, where $(234/d)$ was obtained by fitting the theoretical results for isolated tubes, and $C(N,d)$ is a function that counts for the upshift in bundles, which in turn depends on the number of tubes in a bundle (N) and tube diameter (d). $C(N,d)$ is a refined functional form of the one proposed by Henrard and co-workers:⁴⁸ $C(d) = (10.3d - 2.3)2.56/d(\text{cm}^{-1})$, which results in a much larger upshift of $\sim 25 \text{ cm}^{-1}$, for the range of the diameter tubes considered in this work, than the observed values.⁴⁹

In this work, our calculations were carried out for isolated tubes and ropes with optimized intertube distances. Figures 7 and 8 display RBM results for CNT's and BN-NT's, respectively. We fitted the obtained RBM values to A/R , where R is the radius and A the fitting constant (see Table IV). Note that

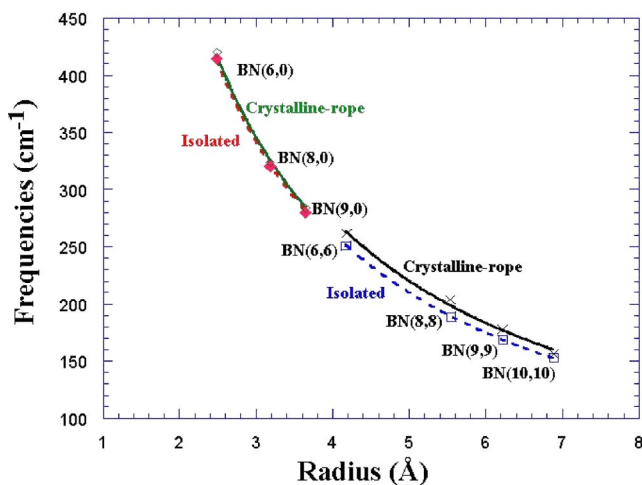


FIG. 8. FP-LCAO BN-NT's RBM's of isolated (dashed lines) tubes and crystalline ropes (solid lines) as a function of tube radius.

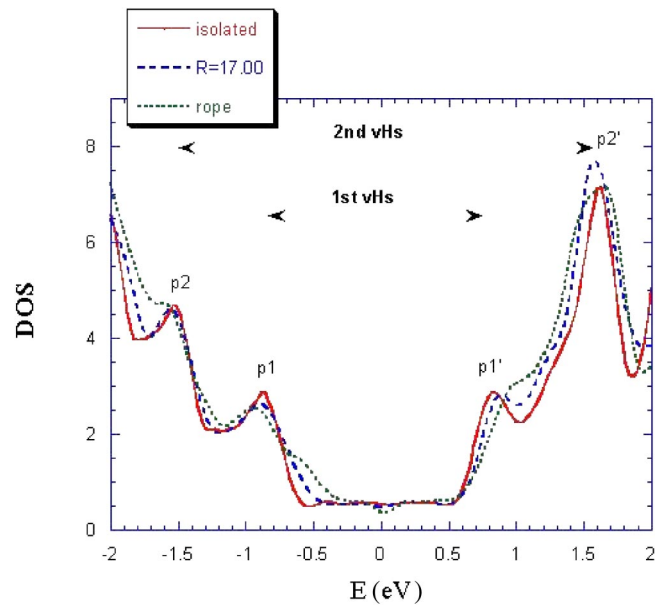


FIG. 9. PW-PP Electronic density of states (DOS) for various intertube distances of the C(10,10) metallic nanotube.

the reported values (Table IV) were converted to $(\text{cm}^{-1} \text{ nm})$ for consistency. Interestingly, our DFT calculations suggest a slight dependency of the RBM's on the chirality for the range of diameters considered in this work (Table I). The CNT's fitting constants results, for isolated tubes, are consistent with previous PW-PP RBM calculations,⁴² with values of 224.0 and $233.4 \text{ cm}^{-1} \text{ nm}$ for the zigzag and armchair tubes, respectively. Furthermore, to assess the reliability of the A/R relationship, in terms of extrapolating results to larger diameter tubes, a DFT calculation for the isolated armchair C(20,20) tube (80 atoms per unit cell) was performed, obtaining a value of 84 cm^{-1} , in good agreement with the extrapolated value of 86 cm^{-1} . These results imply that our fitting constants could be used to predict RBM's for large diameter tubes. A further comparison was made with the proposed model of Bachilo *et al.*²⁴ for isolated semiconducting tubes. Although our armchair-RBM results for isolated tubules fitted well $(224.2/d + 12.5)(\text{cm}^{-1})$ with this model, it does not hold for large diameter tubes, as we obtained an extrapolated value of 92 cm^{-1} for the C(20,20) tube. Furthermore, the additional constant

TABLE IV. Fitting constants of radial breathing modes in crystalline rope and in isolated CNT's and BN-NT's. Units are in $(\text{cm}^{-1} \text{ nm})$.

Chirality	Radial breathing modes fitting constants	
	Crystalline-rope	Isolated
C(n,0)	228.0	224.0(232.0) ^a
C(n,n)	241.4	233.4(236.0) ^a
BN(n,0)	207.6	205.0
BN(n,n)	220.2	209.8

^aReference 42.

TABLE V. Radial breathing modes (cm^{-1}) in crystalline ropes (Rope) and in isolated (Isol.) tubes of CNT's and BN-NT's.

Chirality	C			BN		
	Rope	Isol.	Upshift	Rope	Isol.	Upshift
(6,0)	460.7	453.6	1.5%	420.0	414.5	1%
(8,0)	366.5	361.0	1.5%	320.6	317.1	1%
(9,0)				283.6	279.8	1%
(10,0)	299.5	291.4	2%			
(4,4)	435.0	426.0	2%			
(6,6)	297.0	287.0	3.5%	261.6	251.1	4%
(8,8)	229.0	215.0	6.5%	203.6	188.8	7%
(9,9)				177.7	168.6	5%
(10,10)	181.0	171.0	6%	156.4	153.0	2%

12.5 cm^{-1} has no physical meaning when d tends to infinity, as this frequency vanishes for a flat graphene sheet, corresponding to the $q=0$ transverse acoustic mode.

In BN-NT's, a similar A/R trend has been obtained, with fitting constants lower than those of CNT's by 8 and 10 %, in zigzag and armchair tubes, respectively. Moreover, intertube interactions alter the RBM's, as seen in the increase of their values (Table V) for crystalline ropes. Indeed, we tested the sensitivity of the RBM's with respect to the intertube distance and found that, although intertube distance values are about 3%, on average, smaller than $(2R+3.4 \text{ \AA})$ (see Table I), the calculated RBM for a C(6,6) tube at the graphite interlayer distance (3.4 \AA), for example, was found to equal that of an isolated tube (287.0 cm^{-1}). Thus, the RBM calculations were performed at the optimized intertube distances.

Other theoretical work^{48,49} reported an up shift between 8 and 12 % in the RBM values for C(9,9) and C(10,10) tubes. Our results show lower upshifts, especially in the case of zigzag tubes, where the upshift is found to be small and

systematic, about 2% in CNT's and 1% in BN-NT's, whereas it varies from 2 to 7 % in the armchair CNT's and BN-NT's, as listed in Table V.

Calculations of the electronic density of states of CNT's were carried out to study the change of the first and second vHS due to tube coupling, as compared to a previous tight-binding scheme,⁵⁰ which reported on the effects of intertube interactions on the electronic structures, such as the opening of a pseudogap due to the broken symmetry^{51,52} in metallic C(10,10) nanotubes. The study suggested that the pseudogap expands the vHS, concluding that the expansion needs to be taken into account in the characterization of tubes by Raman spectroscopy. We examined the trend of the vHS in C(6,6), C(8,8), and C(10,10) tubes. Figures 9–11 summarize the electronic DOS, with various intertube distances for each tube. The opening of a pseudogap is shown in all cases, appearing exactly at the equilibrium intertube distance. Interestingly, this pseudogap does not always lead to an outward expansion (away from the Fermi energy) of all vHS. As the tubes are brought together in C(10,10), the vHS peaks

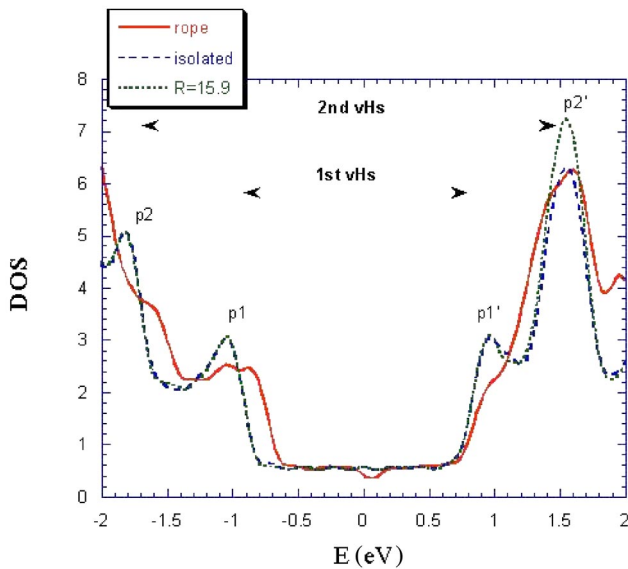


FIG. 10. PW-PP Electronic density of states (DOS) for various intertube distances of the C(8,8) metallic nanotube.

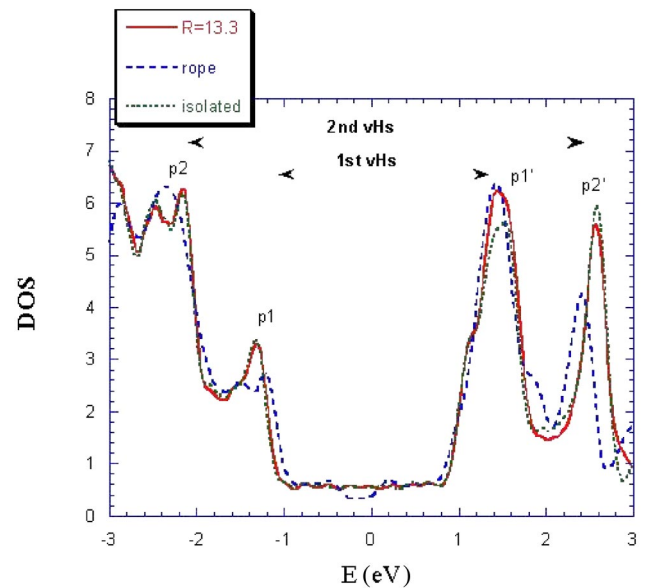


FIG. 11. PW-PP Electronic density of states (DOS) for various intertube distances of the C(6,6) metallic nanotube.

TABLE VI. Results of the first (E_{11}) and second (E_{22}) van Hove singularities for selected crystalline-rope (rope) and isolated (isol.) armchair CNT's. Units are in eV.

	C(6,6)		C(8,8)		C(10,10)	
	Rope	Isol.	Rope	Isol.	Rope	Isol.
E_{11}	2.634	2.850	2.011	1.867	1.977	1.722
E_{22}	4.817	4.733	3.366	3.233	3.255	3.144
E_{22}/E_{11}	1.829	1.661	1.674	1.732	1.646	1.826

broaden, creating a pseudogap at the Fermi level centered at zero, causing an outward expansion of the vHS. However, in the case of C(8,8), an inward shift of the second vHS in the conduction band was obtained. As we proceed to a smaller tube radius, for example C(6,6), the singularities were shifted inward, except for the valence second vHS, which was shifted outward. This is in contrast to the tight-binding results,⁵⁰ where the singularities were predicted to always shift outward when the tubes are brought together. Also, the E_{22}/E_{11} values were found to be, on average, on the order of 1.7 (Table VI) for the armchair tubes, with a value of 2.0 for

the C(10,0) zigzag nanotube, generally in agreement with experiment.²⁶

IV. CONCLUSIONS

A comparative study using first-principle calculations revealed interesting features for BN and C nanotubes, such as the trends in bondlengths, toughness, and RBM's. We reviewed the Young's moduli values in light of recent experimental data. The high sensitivity of the RBM's to the intertube distance has been explored, highlighting the importance of the cell parameters optimization. In addition, we provided a fine analysis of the RBM's trends, comparing our results, in the case of the armchair CNT's, with previously reported models. Finally, we reported on the effects of vHS due to van der Waals interactions, in the armchair CNT's electronic DOS, revealing that the outward expansion of the vHS does not hold for all diameter nanotubes.

ACKNOWLEDGMENTS

We would like to acknowledge the help and support provided by the High Performance Computing Program and the Aeronautical Systems Center Major Shared Resource Center (ASC/MSRC).

- ¹S. Iijima, *Nature (London)* **56**, 345 (1991).
²N. C. Chopra, R. J. Luyken, K. Cherrey, V. H. Crespi, M. L. Cohen, S. G. Louie, and A. Zettl, *Science* **269**, 966 (1995).
³M. A. Reed and J. M. Tour, *Sci. Am.* **282**, 86 (2000).
⁴Z. Yao, H. W. Ch. Postma, L. Balents, and C. Dekker, *Nature (London)* **402**, 273 (1999).
⁵S. J. Tan, A. R. M. Verschuere, and C. Dekker, *Nature (London)* **393**, 49 (1998).
⁶H. W. Ch. Postma, T. Tijs, Z. Yao, M. Grifoni, and C. Dekker, *Science* **293**, 76 (2001).
⁷B. G. Demczyk, Y. M. Wang, J. Cumings, M. Hetman, M. Han, A. Zettl, and R. O. Ritchie, *Mater. Sci. Eng., A* **334**, 173 (2002).
⁸B. I. Yakobson and P. Avouris, *Carbon Nanotubes: Synthesis, Structure, Properties, and Applications*, edited by M. S. Dresselhaus, G. Dresselhaus, and Ph. Avouris (Springer-Verlag, Berlin, 2001), p. 287.
⁹J. P. Lu, *Phys. Rev. Lett.* **79**, 1297 (1997).
¹⁰E. Hernandez, C. Goze, P. Bernier, and A. Rubio, *Phys. Rev. Lett.* **80**, 4502 (1998).
¹¹D. Sanchez-Portal, E. Artacho, J. M. Soler, A. Rubio, and P. Ordejon, *Phys. Rev. B* **59**, 12 678 (1999).
¹²C. A. Cooper, D. Ravich, D. Lips, J. Mayer, and H. D. Wagner, *Compos. Sci. Technol.* **62**, 1105 (2002).
¹³A. C. Dillon, K. M. Jones, T. A. Bekkedahl, C. H. Kiang, D. S. Bethune, and N. J. Heben, *Nature (London)* **386**, 377 (1997).
¹⁴A. G. Rinzler, J. H. Hafner, P. Nikolaev, L. Lou, S. G. Kim, D. Tomanek, P. Nordlander, D. T. Colbert, and R. E. Smalley, *Science* **269**, 1550 (1995).
¹⁵W. A. de Heer, A. Chatelain, and D. Ugarte, *Science* **270**, 1179 (1995).
¹⁶P. G. Collins and A. Zettl, *Appl. Phys. Lett.* **69**, 1969 (1996).
¹⁷R. H. Baughman, A. A. Zakhidov, and W. A. de Heer, *Science* **297**, 787 (2002).
¹⁸X. Blase, A. Rubio, S. G. Louie, and M. L. Cohen, *Europhys. Lett.* **28**, 335 (1994).
¹⁹J. B. Yoo, J. H. Han, S. H. Choi, T. Y. Lee, C. W. Jeong, J. H. Lee, SeGi Yu, GyeongSu Park, W. K. Yi, H. S. Kim, Y.-J. Baik, and J. M. Kim, *Physica B* **332**, 180 (2002).
²⁰R. Saito and H. Kataura, *Carbon Nanotubes: Synthesis, Structure, Properties, and Applications* (Ref. 8), p. 2213.
²¹M. S. Dresselhaus, G. Dresselhaus, A. Jorio, A. G. Souza Filho, and R. Saito, *Carbon* **40**, 2043 (2002).
²²J. -L. Sauvajol, E. Anglaret, S. Rols, and L. Alvarez, *Carbon* **40**, 1697 (2002).
²³J.-C. Charlier and Ph. Lambin, *Phys. Rev. B* **57**, 15 037 (1998).
²⁴S. M. Bachilo, M. S. Strano, C. Kittrel, R. H. Hauge, R. E. Smalley, and R. B. Weisman, *Science* **298**, 2361 (2002).
²⁵B. Akdim, X. Duan, W. W. Adams, and R. Pachter (unpublished).
²⁶M. J. O'Connell, S. M. Bachilo, C. B. Huffman, V. C. Moore, M. S. Strano, E. H. Haroz, K. L. Rialon, P. J. Boul, W. H. Noon, C. Kittrell, J. Ma, R. H. Hauge, R. B. Weisman, and R. E. Smalley, *Science* **297**, 593 (2002).
²⁷DMOL3/CASTEP, Accelrys, Inc.
²⁸Y. Wang, J. P. Perdew, J. A. Chevary, L. D. MacDonald, and S. H. Vosko, *Phys. Rev. A* **41**, 78 (1990).
²⁹M. Kamiya, T. Tsuneda, and K. Hirao, *J. Chem. Phys.* **117**, 6010 (2002).
³⁰E. Engel and A. F. Bonetti, *Int. J. Mod. Phys. B* **15**, 1703 (2001).
³¹L. A. Girifalco and M. Hodak, *Phys. Rev. B* **65**, 125404 (2002).
³²L. A. Girifalco, M. Hodak, and R. S. Lee, *Phys. Rev. B* **62**, 13 104 (2000).
³³W. J. Hehre, L. Radom, P. v. R. Schleyer, and J. A. Pople, *Ab Initio Molecular Orbital Theory* (Wiley, New York, 1986), p. 231.
³⁴Y. Baskin and L. Mayer, *Phys. Rev.* **100**, 544 (1955).

- ³⁵R. S. Pease, *Acta. Crystallogr.* **5**, 356 (1952).
- ³⁶M. M. J. Treacy, T. W. Ebbesen, and J. M. Gibson, *Nature (London)* **381**, 678 (1996).
- ³⁷A. Krishnan, E. Dujardin, T. W. Ebbesen, P. N. Yinilos, and M. M. J. Treacy, *Phys. Rev. B* **58**, 14 013 (1998).
- ³⁸J.-P. Salvetat, G. A. D. Briggs, J.-M. Bonard, R. R. Bacsa A. J. Kulik, T. Stocklin, N. A. Burnham, and L. Forro, *Phys. Rev. Lett.* **82**, 944 (1999).
- ³⁹N. C. Chopra and A. Zettl, *Solid State Commun.* **105**, 297 (1995).
- ⁴⁰G. Zhou, W. Duan, and B. Gu, *Chem. Phys. Lett.* **333**, 344 (2001).
- ⁴¹T. Dumitrica, C. M. Landis, and B. Yakobson, *Chem. Phys. Lett.* **360**, 181 (2002).
- ⁴²J. Kurti, G. Kresse, and H. Kuzmany, *Phys. Rev. B* **58**, R8869 (1998).
- ⁴³G. D. Li, Z. K. Tang, N. Wang, and J. S. Chen, *Carbon* **40**, 917 (2002).
- ⁴⁴H. Kuzmany, B. Burger, A. Thess, and R. E. Smalley, *Carbon* **36**, 709 (1998).
- ⁴⁵L. Alvarez, A. Righi, T. Guillard, S. Rols, E. Anglaret, D. Laplaze, and J.-L. Sauvajol, *Phys. Chem. Lett.* **316**, 186 (2000).
- ⁴⁶S. Bandow, S. Asaka, Y. Saito, A. M. Rao, L. Grigorian, E. Richter, and P. C. Eklund, *Phys. Rev. Lett.* **80**, 3779 (1998).
- ⁴⁷H. Kuzmany, W. Plank, M. Hulman, Ch. Kramberger, A. Gruneis, Th. Pichler, H. Peterlik, H. Kataura, and Y. Achiba, *Eur. Phys. J. B* **22**, 307 (2001).
- ⁴⁸L. Henrard, E. Hernandez, P. Bernier, and A. Rubio, *Phys. Rev. B* **60**, R8521 (1999).
- ⁴⁹U. D. Venkateswaran, A. M. Rao, E. Richter, M. Menon, A. Rinzler, R. E. Smalley, and P. C. Eklund, *Phys. Rev. B* **59**, 10 928 (1999).
- ⁵⁰A. M. Rao, J. Chen, E. Richter, U. Schlecht, P. C. Eklund, R. C. Haddon, U. D. Venkateswaran, Y.-K. Kwon, and D. Tomanek, *Phys. Rev. Lett.* **86**, 3895 (2001).
- ⁵¹P. Delaney, H. J. Choi, J. Ihm, S. G. Louie, and M. L. Cohen, *Nature (London)* **391**, 466 (1998).
- ⁵²P. H. Tan, C. Y. Hu, F. Li, S. Bai, P. X. Hou, and H. M. Cheng, *Carbon* **40**, 1131 (2002).